


 Cite this: *RSC Adv.*, 2023, **13**, 35831

# Biosorption of uranyl ions from aqueous solutions by soluble renewable polysaccharides

 Oshrat Levy-Ontman,<sup>ID</sup>\*<sup>a</sup> Ofra Paz-Tal,<sup>\*b</sup> Yaron Alfi<sup>a</sup> and Adi Wolfson<sup>a</sup>

Polysaccharides derived from natural sources have been offered as environment friendly sorbents for the adsorption of heavy metals. We present a simple technique to remove uranyl ions from aqueous solutions by using representative polysaccharides. The adsorption efficiency of  $\text{UO}_2^{2+}$  decreased in the following order: xanthan gum > kappa > iota/guar gum, for instance, the efficiencies after sorption of 30 min with 500 mg per L uranyl acetate and 0.03 g of the corresponding polysaccharide were: 89.7%, 85.2%, 79.1% and 77.1%. Lowering the acidity in the system decreased the sorption efficiency with all the polysaccharides, and reducing the ratio between the amount of uranyl ions and the amount of polysaccharide increased the sorption efficiencies, e.g., using 500 mg per L uranyl acetate and 0.05 g of the corresponding polysaccharide (xanthan gum, kappa, iota, guar gum) yielded after 30 min sorption efficiencies of 94.3%, 91.5%, 89.0% and 87.7%, respectively. FTIR, SEM-EDS and TGA analyses verified the presence of uranium in the polysaccharides and showed that the uranyl ions were interacting with the different functional groups. Moreover, the addition of uranyl ions to the polysaccharides caused a sharp decrease in viscometry measurements. In addition, the measurements showed that the addition of uranyl lowered both modules,  $G'$  and  $G''$ , and made the solution more liquid.

 Received 24th August 2023  
 Accepted 1st December 2023

DOI: 10.1039/d3ra05794a

[rsc.li/rsc-advances](https://rsc.li/rsc-advances)

## 1. Introduction

Uranium, the heaviest naturally occurring element on Earth, is the primary fuel for nuclear reactors.<sup>1,2</sup> It is also used for other applications, from the space industry to medicine. Uranium ore extraction from the ground and subsequent use as a nuclear fuel leads to the production of large amounts of wastewater that contains uranium ions, mainly as a hexavalent cation ( $\text{U(VI)}$ ).<sup>3,4</sup>

As a radioactive substance, a large amount of uranium, above natural levels, can cause different health effects,<sup>5</sup> such as liver and kidney disease.<sup>6</sup> Moreover, long exposure to uranium radionuclides may also cause cancer.<sup>7</sup> The World Health Organization has therefore listed  $\text{U(VI)}$  as a carcinogen and determined that its concentration in water should not exceed 50 mg L<sup>-1</sup>. Nonetheless, the US Environmental Protection Agency has recommended that 20 mg per L <sup>238</sup>U be set as the standard for drinking water. In addition, wastewater that contains uranium is also hazardous for ecosystems.<sup>8,9</sup> A variety of methods exist for the removal from wastewater of uranium or uranyl ions ( $\text{UO}_2^{2+}$ ), the latter formed by the hydrolysis of uranium.<sup>3,4,10,11</sup> The most studied and applicable methods are extraction,<sup>12–14</sup> flotation,<sup>15,16</sup> precipitation,<sup>17,18</sup> membrane filtration,<sup>19,20</sup> electro dialysis<sup>21</sup> and adsorption.<sup>22–27</sup> Among these

techniques, adsorption based on different organic and inorganic adsorbents was found to be the simplest, most effective and most versatile method.

Biosorbents, living or dead biomass (e.g., algae, yeast and bacteria) and their derived products, such as polysaccharide-based materials, have also been shown to adsorb different contaminants from wastewater, among them radioactive ions,<sup>28</sup> including uranium.<sup>26,29</sup> Insofar as they are renewable, biodegradable and usually hydrophilic polymers, polysaccharides produced from biological sources are considered safe for use. As such, they have numerous applications,<sup>30</sup> including in the food,<sup>31</sup> pharmaceuticals<sup>32</sup> and cosmetics<sup>33</sup> industries. This wide applicability is due to the variability in the characteristics of each polysaccharide, which depends on its functional groups and its structure. Among its other qualities, these properties also render them good adsorbents for heavy metal ions.<sup>34–36</sup> Moreover, they are readily available and usually more cost-effective than synthetic adsorbents.

Different polysaccharide-based systems have been used to remove  $\text{U(VI)}$  from aqueous solutions that resemble wastewater. For example, Marqués *et al.* reported that exopolysaccharide from *Pseudomonas* sp. was able to remove uranium from an aqueous solution with a maximum uptake of 96 µg U per mg polymer.<sup>37</sup> In addition, Kazy *et al.* used extracellular polysaccharide (EPC) produced by a *Pseudomonas aeruginosa* strain to remove uranium from an aqueous solution.<sup>38</sup> The maximum sorption observed was 985 mg U per g polymer at pH 5.0 due to the strong binding of uranium with the carboxylic groups of the

<sup>a</sup>Department of Chemical Engineering, Shamon College of Engineering, Basel/Bialik Sts., Beer-Sheva 8410001, Israel. E-mail: oshrale@sce.ac.il; Tel: +972-8-6475636

<sup>b</sup>Nuclear Research Center, Negev, Beer-Sheva 84190, Israel. E-mail: ofrapt@gmail.com; Tel: +972-8-6567514



uronic acids in the polymer, while at lower pH values, amino and hydroxyl groups were responsible for the bulk of metal binding. Sakaguchi *et al.* studied the adsorption of uranium from seawater by titanium(IV)-cellulose-xanthate or titanium(IV)-starch-xanthate, which yielded an uptake of about 77% when 1 g of the adsorbent was suspended in 5 L of natural seawater with constant stirring at 30 °C for three days.<sup>39</sup> In later work, alginate beads that were prepared in a CaCl<sub>2</sub> solution were successfully used for uranium recovery from aqueous solutions. The adsorption efficiency and distribution constant ( $K_d$ ) for uranium ions under optimized experimental conditions were  $91 \pm 1\%$  and  $10\,043 \pm 834 \text{ mL g}^{-1}$ , respectively.<sup>40</sup> In other studies, a chitosan-glucan complex<sup>41</sup> and different cross-linked chitosan systems,<sup>41–43</sup> which were insoluble in wastewater, and a magnetic biosorbent composed of nanoparticles of magnetite covered with chitosan,<sup>44</sup> were also successfully tested. Furthermore, water insoluble polysaccharides like chitin and chitosan were also shown to be efficient biosorbents.<sup>45,46</sup>

In this study, we report on the sorption of  $\text{UO}_2^{2+}$  from aqueous solutions using natural and water-soluble polysaccharides as adsorbents. The separation process is very fast and straightforward, and the adsorption capacities, which were detected after precipitation and filtration of the different polysaccharides with the uranyl ions, were effective and dependent on polysaccharide type.

## 2. Experimental

### 2.1 Materials

All of the polysaccharides used in this study (guar gum (G), xanthan gum (X), iota (I), kappa (K)), uranyl acetate dihydrate ( $\text{UO}_2(\text{CH}_3\text{COO})_2 \cdot 2\text{H}_2\text{O}$ ), and other chemicals (analytical grades) were purchased from Sigma-Aldrich.

### 2.2 Preparation of polysaccharide solutions

One g of polysaccharide (G/X/I/K) was dissolved in 100 mL double-distilled water (DDW) and mixed for 1 h, yielding 1% w/v aqueous solution of polysaccharide. When I and K were used, the mixture was heated to 50 °C and stirred for another 1 h.

### 2.3 Sorption experiments

In a typical procedure, 1–5 mL of 1% w/v aqueous solution of polysaccharides were added to 5–9 mL of an aqueous solution of  $\text{U}(\text{VI})$  (500–900  $\text{mg L}^{-1}$ ), which were prepared from a uranyl acetate stock solution of 1000  $\text{mg L}^{-1}$  via proper dilution, and then mixed for 30 min at room temperature. (In all of the experiments, the final volume was 10 mL). Then,  $4 \times 10 \text{ mL}$  of cold ethanol was added to the aqueous solution, after which the solution was mixed and the solid was removed by centrifugation and filtration. It worth mentioned that the amount of ethanol that used to allow full and ease separation of the polysaccharide and the  $\text{UO}_2^{2+}$  ion within it, should be optimized to make the system more sustainable. Finally, the ethanol was evaporated from the solution, and the concentration of  $\text{U}(\text{VI})$  that was left in the solution was detected using ICP-OES (SPECTRO, model ARCOS, error limit  $\pm 10\%$ ) and UV-Vis analysis (Agilent, model

8453, wavelength accuracy  $< \pm 0.5 \text{ nm}$ ) using xylenol orange as indicator.<sup>47</sup>

Each sorption experiment was performed five times, and each displayed yield is the mean of five experiments. In addition, two control sets, one containing only the uranyl solution at an appropriate concentration and the other with the polysaccharides and without the uranyl solution, were also run for comparison.

The sorption efficiency was calculated as follows:

$$\text{Sorption efficiency (\%)} = 100 \times \frac{C_{\text{in}} - C_{\text{f}}}{C_{\text{in}}}$$

where  $C_{\text{in}}$  and  $C_{\text{f}}$  are the initial and final concentrations ( $\text{mg L}^{-1}$ ), respectively, of  $\text{U}(\text{VI})$ .

## 2.4 Characterization methods

**2.4.1 Fourier-transform infrared (FTIR) analysis.** The chemical bonds on the surface of the pristine lyophilized polysaccharides and the pellets that were obtained after the sorption experiments and freeze-dried overnight were recorded with an FTIR system (Nicolet 6700, Thermo Scientific, Waltham, MA, USA) with an attenuated total reflectance (ATR) accessory outfitted with a diamond crystal. The recorded spectra were the means of 36 spectra taken in the  $650\text{--}4000 \text{ cm}^{-1}$  range with a  $0.5 \text{ cm}^{-1}$  resolution, and atmospheric correction was switched on at 25 °C.

**2.4.2 Scanning electron microscope (SEM) and energy dispersive X-ray spectrometry (EDS) analyses.** A scanning electron microscope (SEM, version 460L) with a backscatter electron detector (EDS) equipped with an energy-dispersive X-ray spectroscopy detector (Thermo Fisher) was used to observe the morphology and structure of each polysaccharide before and after  $\text{UO}_2^{2+}$  ion adsorption. The acceleration voltage was 15 kV, and the sample pressure was 60 Pa.

**2.4.3 Thermogravimetric (TGA) analysis.** The thermogravimetric analysis was performed by a thermal analyzer (TGA Q500, TA Instruments), and the recorded thermographs were carried out with nitrogen gas ( $\text{N}_2$ ) as the carrying gas. The samples used for TGA analyses were taken at the completion of batch sorption tests. After centrifugation, the solid portion of each mixture was taken and freeze-dried overnight to remove residual liquid. The sample was subjected to a heating rate of  $10 \text{ °C min}^{-1}$  and a flow of  $90 \text{ mL min}^{-1}$  over a heating range of  $20\text{--}1000 \text{ °C}$ . The changes in weight were plotted as a function of temperature. Repeated tests revealed that the maximum relative error could be controlled to a value below 10%.

**2.4.4 Rheological measurements.** The viscosity of the aqueous samples that contained 0.3% w/v polysaccharide with or without 700 mg per L uranyl ions (final volume of  $\sim 10 \text{ mL}$ ) after 48 h of cooling at 4 °C was determined using a HAAKE RotoVisco 1 rheometer (Thermo Scientific) equipped with an extended temperature cell for temperature control using a stainless-steel cone and plate system ( $d = 60 \text{ mm}$  and  $\theta = 0.5^\circ$ ). The solutions were measured at 25 °C as a function of the shear rate in an upward sweep from 1 to  $1000 \text{ s}^{-1}$ . The oscillatory shear experiments were carried out using a rheometer TA



AR2000 (TA Instruments, New Castle Delaware, USA) equipped with an extended temperature cell for temperature control and stainless-steel parallel plate ( $d = 40$  mm). The dynamic viscoelastic characterization of the solutions was determined by the frequency dependence (between 0.05 and 20 Hz) of the storage and loss moduli,  $G'(\omega)$  and  $G''(\omega)$ , respectively, at 25 °C.

### 3. Results and discussion

The nature of the polysaccharide, *i.e.*, its structure and the functional groups on its backbone, and the characteristics of the ion to be removed, *i.e.*, its size and charge, are used to detect the ion sorption efficiency. Recently, we proposed a novel method for the recovery of europium ions ( $\text{Eu}^{3+}$ ) from aqueous solutions by adding an aqueous solution of readily available, commercial polysaccharides to a europium solution.<sup>48</sup>  $\text{Eu}^{3+}$ , which could associate with the sulfate, carboxylic and hydroxyl groups on the backbone of the polysaccharide, was preferably adsorbed to the more acidic groups. Thus, it was suggested that the same method can also be employed with renewable polysaccharides to recover  $\text{UO}_2^{2+}$  ions from aqueous solutions.

The sorption of  $\text{UO}_2^{2+}$  was investigated by using four representative polysaccharides with different functional groups: G with only hydroxyl groups, X with hydroxyl and carboxylic groups, and carrageenan types I and K with hydroxyl and ester sulfate groups. As  $\text{UO}_2^{2+}$  sorption efficiency reached equilibrium after 30 min, the investigation began with a study of the effects of both the  $\text{UO}_2^{2+}$  concentration and the amount of polysaccharide on the sorption efficiency after 30 min at 298 K and  $\text{pH} = 4.5$ . The results in Table 1 show that at polysaccharide amounts of 0.03 g and above, X exhibited the highest sorption efficiency, followed by K with slightly lower yields, while the use of I and G resulted in additional small decreases in the sorption efficiency under all the conditions. As previously noted, the difference in sorption efficiency between the four polysaccharides might be attributed to the different functional groups on the polymers. The carboxylic groups on X seem to be slightly more effective sorption agents of  $\text{UO}_2^{2+}$  compared to the ester sulfate groups and the hydroxyl on the two carrageenans and to the hydroxyl groups in G. In addition, surprisingly, K, which has one sulfate ester group, exhibited higher sorption efficiencies than I, which has two sulfate groups. This finding may be explained by the different molecular structure of the two carrageenans – though both polysaccharides form three-fold, right-handed double helice conformations composed of parallel chains, I has a longer helix pitch than K, and the chain positions differ significantly. In addition, I forms weaker and more elastic gels than K,<sup>49,50</sup> which may affect the functional group availability.<sup>51</sup> Notably, the higher sorption efficiencies attributed to K compared to that of I differ from our former findings, which demonstrated that I is a better  $\text{Eu}^{3+}$  sorbent than K.<sup>48,51</sup> The observed differences in sorption behaviour are the manifestation of the dependence of that behaviour on both the nature of the polysaccharide and the characteristics of the metal ions.

As expected, all four polysaccharides exhibited higher sorption efficiencies when the metal concentration in the solution

Table 1 Sorption efficiencies of representative polysaccharides

Polysaccharide	Sorption efficiencies (%) $\pm$ 3%			
	U(vi) (mg L <sup>-1</sup> ): PS (g)			
	900 : 0.01	500 : 0.05	700 : 0.03	500 : 0.03
Guar gum (G)	57.9	87.7	77.1	82.2
Iota (I)	58.9	89.0	79.1	80.7
Kappa (K)	66.7	91.5	85.2	88.9
Xanthan gum (X)	65.4	94.3	89.7	95.0

was lower or when the polysaccharide amount was higher (Table 1). This observation implies that reducing the  $\text{UO}_2^{2+}$ /polysaccharide ratio increased the sorption efficiency, as the number of adsorbing functional groups on the polysaccharide relative to the number of adsorbed ions increased. Above a concentration of 700 mg L<sup>-1</sup>, however, it seems that there are not enough available binding sites in the polysaccharides, thus causing the yields to decline markedly. As such, in solutions that contained a high uranyl concentration (900 mg L<sup>-1</sup>) and a low amount of polysaccharides (0.01 g), the sorption efficiencies that were detected for G, I, K, and X were 57.9%, 58.9%, 66.7%, and 65.4%, respectively (Table 1).

The adsorption kinetics of the two polysaccharides that exhibited the highest sorption efficiencies, X and K, were determined by using a pseudo-first order and a pseudo-second order kinetic models. The expressions of the two models after linearization are given in eqn (1) and (2), respectively, where  $q_t$  and  $q_e$  are the uranyl adsorption capacity (mg g<sup>-1</sup>) at any time  $t$  (min) and at equilibrium, and,  $k_1$  (min<sup>-1</sup>) is pseudo-first order rate constant and  $k_2$  (g mg<sup>-1</sup> min<sup>-1</sup>) is pseudo-second order rate constant.

$$\ln(q_e - q_t) = \ln(q_e) - k_1 t \quad (1)$$

$$\frac{t}{q_t} = \frac{t}{q_e} + \frac{1}{k_2 q_e^2} \quad (2)$$

The results of modelling are presented in Fig. 1. It can be seen that the sorption with both polysaccharides fits to pseudo-second order model (with high  $R^2$  values) indicating that chemisorption is the rate-limiting mechanism of the process, and that uranyl was chemically adsorbed to the polysaccharides.

#### 3.1 FTIR analysis

ATR-FTIR spectroscopy was used to gain knowledge about the interaction between the  $\text{UO}_2^{2+}$  and the different functional groups on the polysaccharides, before and after the sorption, the latter of which is designated as U-PS (polysaccharide), *e.g.*, the I after adsorption of  $\text{UO}_2^{2+}$  ions was labelled U-I.

ATR-FTIR spectra of pristine G *vs.* U-G are shown in Fig. 2. As expected, the spectrum of pristine G contains the typical bands in accordance with the G structure: a broad band assigned to the -OH stretching at 3333 cm<sup>-1</sup>; a peak at 2920 cm<sup>-1</sup> that confirmed -CH<sub>2</sub>- asymmetric stretching



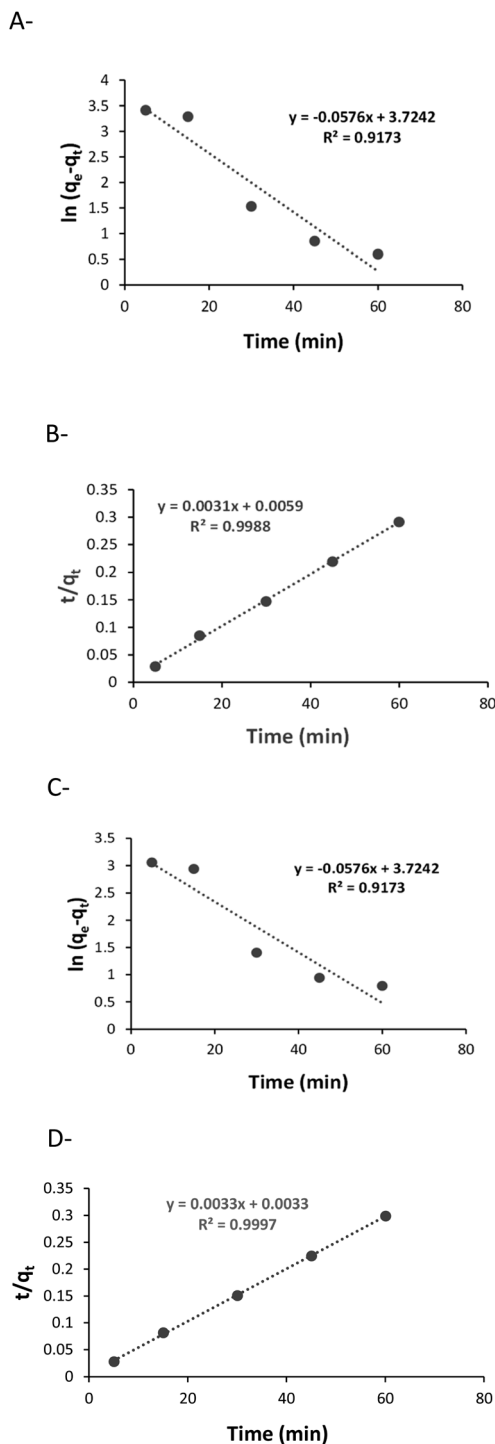


Fig. 1 Kinetics of uranyl sorption: (A) pseudo-first order with X, (B) pseudo-second order with X, (C) pseudo-first order with K, (D) pseudo-second order with K.

vibrations; and a peak at  $1403\text{ cm}^{-1}$  that confirmed the C-H stretching vibrations.<sup>52</sup> In addition, the ring stretching of mannose and bending vibration of the OH group and associated water molecules were observed at  $1640\text{ cm}^{-1}$  and the  $-\text{CH}_2-$  deformation at  $1384\text{ cm}^{-1}$ . Finally, the peaks in the spectrum between  $863$  and  $1151\text{ cm}^{-1}$  indicated the highly

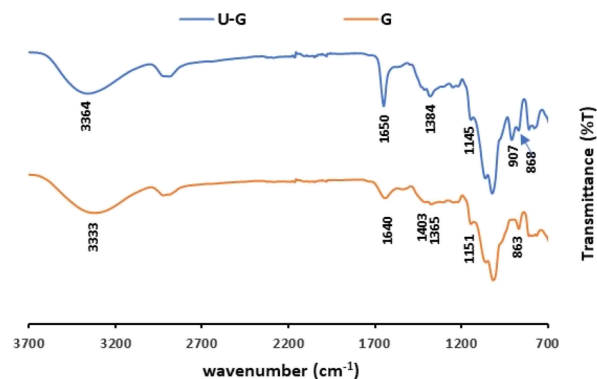


Fig. 2 ATR-FTIR spectra of pristine G and U-G (sorption conditions:  $700\text{ mg per L UO}_2^{2+}$ ,  $3\text{ mL of } 1\% \text{ w/v G}$ ).

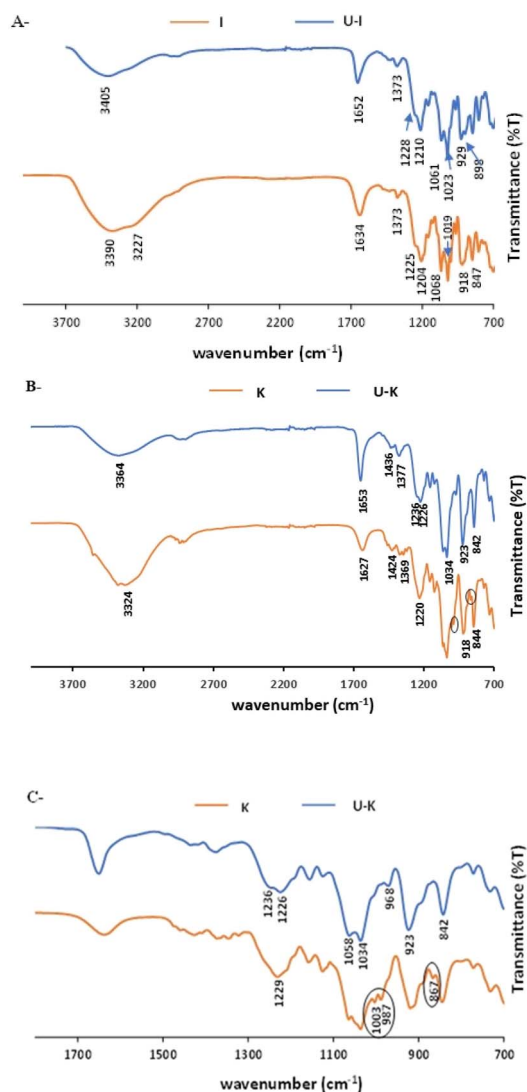


Fig. 3 ATR-FTIR spectra of pristine polysaccharides and their analogues: (A) I and U-I, (B) K and U-K in the range of  $700-3800\text{ cm}^{-1}$ , and (C) K and U-K in the range of  $700-1800\text{ cm}^{-1}$ . (Sorption conditions:  $700\text{ mg per L UO}_2^{2+}$ ,  $3\text{ mL of } 1\% \text{ w/v polysaccharide}$ ).



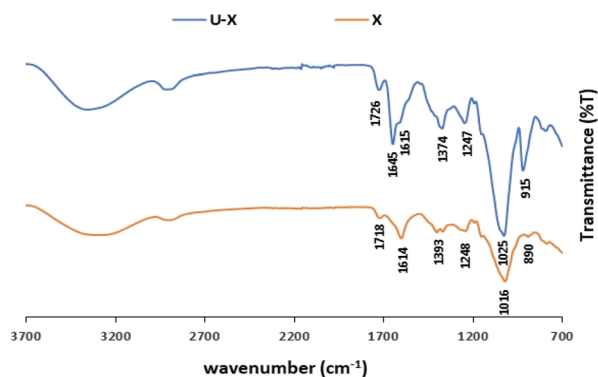


Fig. 4 ATR-FTIR spectra of pristine X and U-X (sorption conditions: 700 mg per L  $\text{UO}_2^{2+}$ , 3 mL of 1 w/v% X).

coupled stretching vibrations of C–O–C, C–C–O, C–OH, and (1–4) and (1–6) linkages of galactose and mannose units.<sup>53,54</sup> Yet when  $\text{UO}_2^{2+}$  ions were adsorbed to the G (U–G, in Fig. 2), the broad peak at  $1640\text{ cm}^{-1}$  shifted to  $1650\text{ cm}^{-1}$  and became sharper, and the peak at  $1151\text{ cm}^{-1}$  shifted to  $1145\text{ cm}^{-1}$ . These changes indicate that the hydroxyl groups of C–OH and  $\text{UO}_2^{2+}$  interacted with each other. Moreover, a new U–G band was observed at  $907\text{ cm}^{-1}$ , which is attributed to O–U–O stretching, also indicating that the metal ions were adsorbed *via* the hydroxyl groups on the polysaccharide.

The FTIR spectra of pristine I and K and their corresponding analogues, U–I and U–K, are shown in Fig. 3. As expected, in their pristine states, the two polysaccharides present the same characteristic bands that are indicative of the basic chemical bonding in the carrageenans, specifically: a peak at  $3200\text{--}3400\text{ cm}^{-1}$  due to the assigned hydrogen O–H stretching vibration bonds; C–O–C of 3,6-anhydro-D-galactose at  $1068\text{ cm}^{-1}$  and  $929/923\text{ cm}^{-1}$ , respectively; O– $\text{SO}_3$  stretching vibration at D-galactose-4-sulfate for I and K at  $1373/1424\text{ cm}^{-1}$  and  $844/847\text{ cm}^{-1}$ , respectively; and at  $804\text{ cm}^{-1}$  for D-galactose-2-sulfate.<sup>55,56</sup> However, following  $\text{UO}_2^{2+}$  sorption, the H–O–H deformation bands of I and K at  $1634\text{ cm}^{-1}$  and  $1627\text{ cm}^{-1}$ , respectively, shifted to  $1652\text{ cm}^{-1}$  and  $1653\text{ cm}^{-1}$ , respectively.<sup>57</sup> Also note that the bands at  $3200\text{--}3500\text{ cm}^{-1}$  that were observed following the addition of  $\text{UO}_2^{2+}$  and that correspond to the O–H stretching vibrations were less intense than those observed in both of the pristine polysaccharides. The reduction in the band intensities could be attributed to reduced hydrogen bonds. Indeed, the interaction of the uranyl ions with the oxygen of the hydroxyl groups can lead to the lower availability of the OH groups that could otherwise self-assemble the polymer chains. In the  $1100\text{--}1300\text{ cm}^{-1}$  range, the characteristic S=O band of the ester sulfate (O=S=O symmetric vibration), which appears in pristine I at  $1204\text{ cm}^{-1}$  and in pristine K at  $1220\text{ cm}^{-1}$ , shifted to a higher wavenumber of  $1210\text{ cm}^{-1}$  in U–I and to double peaks at  $1226\text{ cm}^{-1}$  and  $1236\text{ cm}^{-1}$  in U–K.<sup>58</sup> For O– $\text{SO}_3$  stretching vibrations at D-galactose-4-sulfate, the broad peak of pristine I at  $918\text{ cm}^{-1}$  split into two sharp peaks at  $929$  and  $898\text{ cm}^{-1}$  in U–I. These findings indicate that the  $\text{UO}_2^{2+}$  is also interacting with the ester sulfate groups. Moreover, the band at  $987\text{ cm}^{-1}$ , which corresponds to

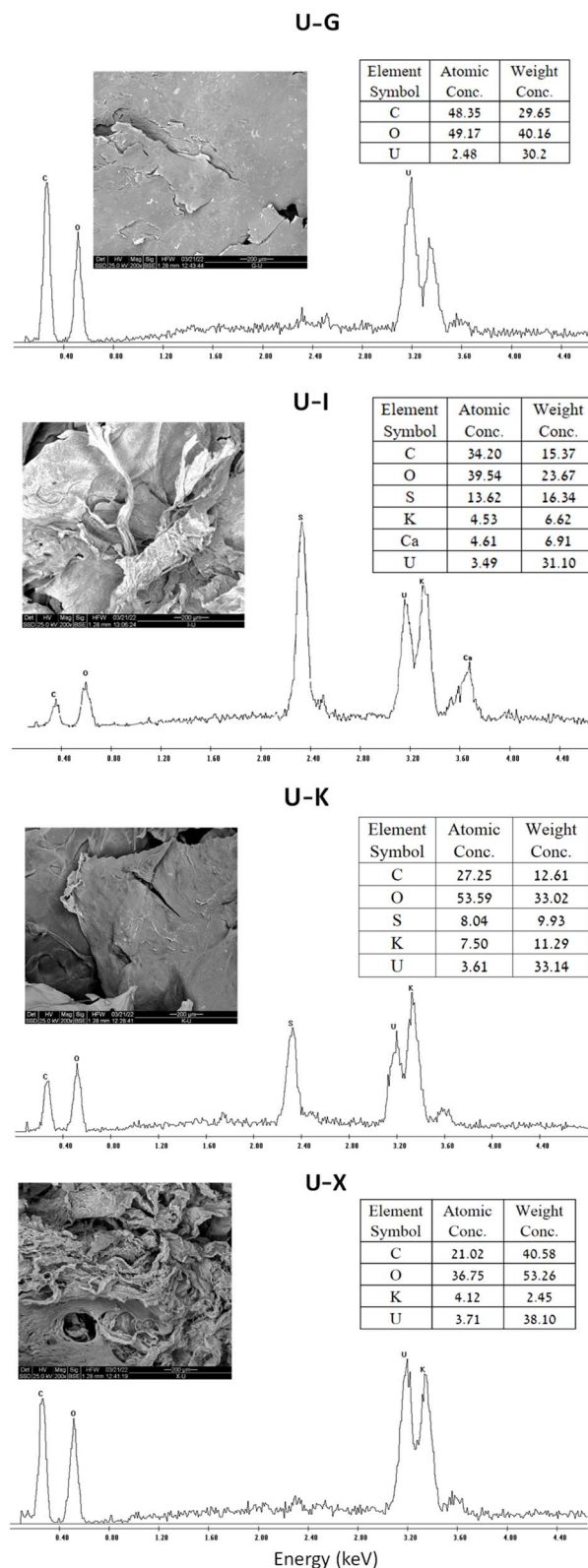


Fig. 5 SEM image at  $\times 200$  magnification, EDS spectrum and tabulated results of polysaccharides before and after  $\text{UO}_2^{2+}$  adsorption (sorption conditions: 700 mg per L  $\text{UO}_2^{2+}$ , 3 mL of 1% w/v polysaccharide).



Table 2 Thermal properties of polysaccharides before and after  $\text{UO}_2^{2+}$  adsorption<sup>a</sup>

Step	G			U-G		
	Onset temp. (°C)	DTG (°C)	Wt loss (%)	Onset temp. (°C)	DTG (°C)	Wt loss (%)
Step 1	—	73.55	6.02	—	79.01	3.85
Step 2	149.61	314.90	80.66	166.75	268.91	37.93
Step 3	—	—	—	318.06	334.20	20.43
Residue			13.31		404.85	37.75
	X			U-X		
Step 1	—	114.64	4.36	—	68.85	6.23
Step 2	176.84	275.17	65.68	154.65	273.19	33.55
Step 3	—	—	—	350.34	348.39	11.07
Step 4	—	—	—	600.5	857.25	6.04
Residue			29.94			43.14
	I			U-I		
Step 1	—	87.44	6.92	—	71.49	9.67
Step 2	137.24	164.84	25.02	156.67	222.92	18.59
Step 3	184.98	256.15	12.81	300.91	356.73	6.87
Step 4	307.36	351.05	12.11	393.72	443.93	10.29
Step 5	599.95	747.71	16.61	509.72	601.06	13.26
Residue			26.54			37.05
	K			U-K		
Step 1	—	69.19	9.31	—	76.24	7.07
Step 2	146.58	259.39	22.39	156.67	278.44	28.40
Step 3	277.71	321.94	23.10	395.73	440.94	22.82
Step 4	500.64	747.92	17.04	—	—	—
Residue			28.16			41.72

<sup>a</sup> Sorption conditions: 700 mg per L  $\text{UO}_2^{2+}$ , 3 mL of 1% w/v polysaccharide.

pristine K, shifted to a lower frequency ( $968\text{ cm}^{-1}$ ) after sorption, and the peak at  $867\text{ cm}^{-1}$ , which corresponds to galactose-4-sulfate, was not observed. Therefore, it can be suggested that the ester sulfate groups were involved in the complexation of the uranyl ions to the K matrix.

The ATR-FTIR spectra of pristine X and U-X are shown in Fig. 4. As expected, the spectrum of pristine X contains bands in the region of  $850\text{--}950\text{ cm}^{-1}$  corresponding to the skeleton mode of the anomeric configuration and glycosidic linkages. It also contains several other typical bands: at  $3310\text{ cm}^{-1}$ , which is due to the O-H axial deformation; at  $2850\text{--}2910\text{ cm}^{-1}$  that is attributed to the symmetric and asymmetric stretching vibrations of the C-H group in the methyl and methylene groups; at  $1718\text{ cm}^{-1}$  due to the C=O stretching ester vibrations; and at  $1614\text{ cm}^{-1}$  and  $1393\text{ cm}^{-1}$  corresponding to asymmetrical and symmetrical stretching vibrations of carboxylate ion, respectively. As illustrated in Fig. 3, the  $1016\text{ cm}^{-1}$  band, which is related to C-O stretching of primary alcohols,<sup>59</sup> shifted to  $1025\text{ cm}^{-1}$  after  $\text{UO}_2^{2+}$  sorption. In addition, a new band appears in U-X, at  $1645\text{ cm}^{-1}$ , assigned to C=O stretching vibrations from pyruvate. These bands indicate that the adsorption caused changes in the axial deformation of the C-O part of the enols, which may indicate interaction of the  $\text{UO}_2^{2+}$  *via* the carboxylic groups. Moreover, the band at  $1393\text{ cm}^{-1}$ , which corresponds to the C-O symmetric stretching of the carboxylate anion,<sup>60</sup> broadened after binding to  $\text{UO}_2^{2+}$ , an observation that may be due to the intermolecular hydrogen bonds between the polysaccharide chains. Furthermore, after

sorption of the metal ions, a new peak appears at  $915\text{ cm}^{-1}$  that can be assigned to the bending vibration of  $\delta\text{U-OH}$ , the asymmetric stretching vibration of  $\nu_3$ ,<sup>61</sup> which might implies on interactions between uranyl ions and OH of carboxyl group, or as in G, the same part of  $\text{UO}_2^{2+}$  was adsorbed *via* the hydroxyl groups on the polysaccharide.

As noted previously in the literature, the nature of metal ion coordination with the different functional groups on the polysaccharides varies among the different ions, and it is also altered by the metal ion concentration in the solution and by the solution pH.<sup>62,63</sup> We also found that, compared to the carboxylic groups on X and the hydroxyl groups on G,  $\text{Eu}^{3+}$  had stronger electrostatic interactions with the ester sulfate groups of I, and at low pH values, increased functional group protonation led to decreased sorption efficiencies.<sup>48</sup> However, as the ionic radius of  $\text{UO}_2^{2+}$  is larger and its charge differs from that of  $\text{Eu}^{3+}$ , it probably interacts differently with the different functional groups. In addition, polysaccharide structure can also affect its sorption ability. As such, higher sorption efficiencies were obtained for X, which not only has different functional groups compared to those of the other tested polysaccharides, also possesses branched glycan residues with carboxylic groups on its backbone that are more available to adsorb uranyl ions.

### 3.2 SEM-EDS analysis

SEM-EDS analysis also confirmed that the metal ions are adsorbed to the different polysaccharides (Fig. 5). As expected,



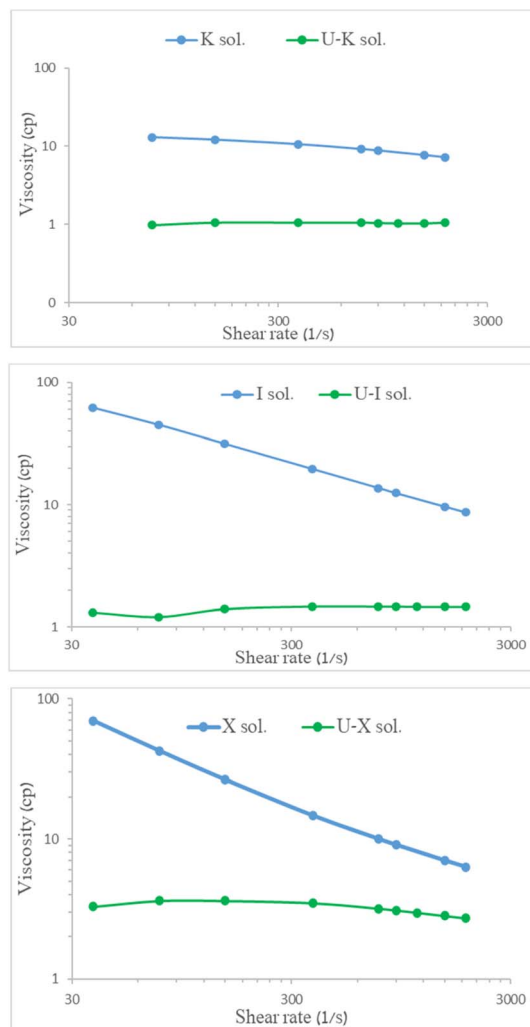


Fig. 6 Viscosity of 0.3% w/v polysaccharides before and after  $\text{UO}_2^{2+}$  adsorption at 25 °C as function of shear rate.

all of the U-polysaccharide composites contain mainly carbon (C) and oxygen (O) from the native polymer and potassium (K) and/or calcium (Ca) as counter ions to the acidic groups on the polysaccharides. In addition, in all of the samples, relatively high amounts of uranium  $\text{U(VI)}$  were also detected in relative contents that are in agreement with the results of the sorption experiments:  $\text{X} > \text{K} > \text{I/G}$ .

### 3.3 TGA analysis

TGA and TG-DTA (differential thermal analysis) analyses of the four polysaccharides (G/X/I/K) before and after  $\text{UO}_2^{2+}$  sorption is presented in Table 2, which summarizes the percentage of mass loss for each stage (% wt loss), the onset temperature and the differential thermogravimetric DTG.

In general, the TGA thermograms of the different polysaccharides, before and after  $\text{UO}_2^{2+}$  sorption, present the same mass weight trend. In the first stage, the water desorption stage, at temperatures below 200 °C, the total weight declined by about 5–10%.<sup>64</sup> This step, mainly due to the interactions between the water molecules and the hydroxyl groups on the

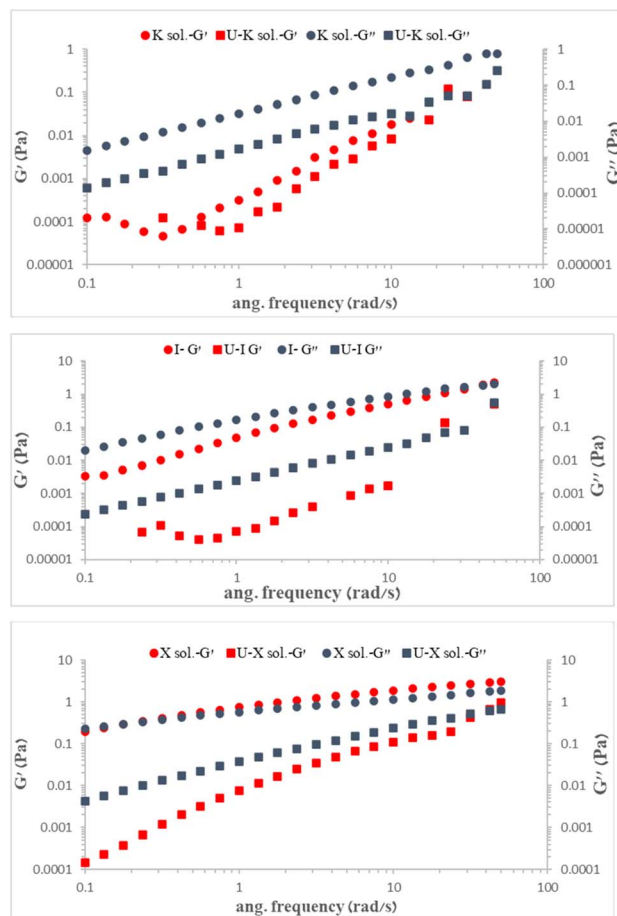


Fig. 7 ( $G'$ ) and ( $G''$ ) modulus of 0.3% w/v polysaccharides before and after  $\text{UO}_2^{2+}$  adsorption at 25 °C.

surface of the polymer backbone, confirms the hydrophilic character of the various polysaccharides. The second stage, at temperatures above 200 °C, involves several steps wherein the polysaccharides decompose until their residue reached a constant mass (~50–80% weight loss) up to ~350 °C. This is attributed to the carbohydrate backbone fragmentation and to the de-polymerization process. For the carrageenans (I and K), these degradation steps are also associated with the degradation of the sulfate ester groups from the pendant chains attached to the polymeric backbone.<sup>65,66</sup> Furthermore, for K and I, a third stage was observed above 700 °C (step 5) that may be due to the decomposition of inorganic salts.<sup>67</sup>

The TGA and TG-DTA curves of all of the polysaccharides after sorption of  $\text{UO}_2^{2+}$  showed higher thermal stability, and the residue after sorption for X, K, I and G increased from 29.94% to 43.14%, 28.16% to 41.72%, 26.54% to 37.05%, and 13.31% to 37.75%, respectively. The main difference observed in thermal behavior was in stage 2, the so-called degradation stage, during which the main pyrolytic process occurred and different volatile components were gradually released. These results suggest that the polysaccharides become more thermally stable after sorption.<sup>68</sup>



Furthermore, the maximum decomposition peaks of K and I shifted to higher temperatures after  $\text{UO}_2^{2+}$  sorption, as reflected in the maximum peak in the DTG curves: 259.39 °C to 278.44 °C and 164.84 °C to 222.99 °C, respectively. This finding may be ascribed to the loss of  $-\text{OSO}_3-$  and  $\text{UO}_2^{2+}$  groups and may also be due to the carbohydrate backbone fragmentation. The temperature for G, however, decreased after sorption from 314.90 °C to 268.97 °C, and for X, a minor change was observed, from 275.17 °C to 273.19 °C. This finding implies that changes occurred in the molecular structures of X and G, and indeed, the ordered or disordered state of X chains is known to be controlled by temperature and ionic strength.<sup>69</sup> It would therefore seem that, after sorption, thermal changes are caused by weak intramolecular interaction forces (e.g., hydrogen bonds). Notably, after the sorption process, all of the polysaccharides exhibited a new, broad peak in the range of 300–400 °C that may be attributed to the decomposition of uranyl in the sample.

The thermal decomposition of uranyl acetate, which was used as the source of uranyl in this study, is known to take place at temperatures between 260 °C and 370 °C.<sup>70,71</sup> This decomposition stage could be due to the fission of the  $\text{UO}_2-\text{O}$  bonds and to the release of the acetate group from the complex, which can also produce acetate radicals.<sup>71</sup> X-ray powder diffraction analysis of the decomposition residues show that in air, uranyl acetate decomposes to U, whereas in nitrogen, the product is mainly non-stoichiometric  $\text{UO}_2^{x+}$ , with small amounts of U. Thus, as the uranyl was adsorbed to the various polysaccharides, without the acetate counter ion, it can be concluded that the peak in the range of 300–400 °C in the U-polysaccharide samples is due to the decomposition of uranyl in the sample that decomposes to U.

### 3.4 Physicochemical analysis

Viscosity measurements of the aqueous polysaccharide solutions (X/I/K sol.) before adsorption and following 30 min of mixing with 700 mg per L uranyl acetate (U-X sol./U-I sol./U-K sol.) are shown in Fig. 6. Notably, measuring the viscosity of the U-G sol. was not applicable because the solution was not homogeneous and contained particles. All of the aqueous pristine polysaccharides yielded typical non-Newtonian fluid behavior, indicating that shear stress reduces the viscosity, whereas the viscosity measurements of the solutions of the U-polysaccharide preparations indicated that all of the preparations lost their high viscosity behavior.

To compare the changes that were obtained for each polysaccharide due to  $\text{UO}_2^{2+}$  adsorption, the mechanical properties of each polysaccharide before and after adsorption, *i.e.*, the storage (or elastic) modulus ( $G'$ ) and viscous (or loss) modulus ( $G''$ ), were measured as functions of the angular frequency (Fig. 7).

As expected, the presence of uranyl ions reduced both modules,  $G'$  and  $G''$ , in the K, I, and X polysaccharides, with  $G'' > G'$ , indicating electrostatic repulsion caused by  $\text{UO}_2^{2+}$  adsorption and distancing of polysaccharide chains. We suggest that the  $\text{UO}_2^{2+}$  reduced the level of entanglement of the polysaccharides while also increasing the free volume between the chains, thereby lowering both  $G'$  and  $G''$ .

## 4. Conclusions

The discharge of industrial wastewater containing heavy metals, and in particular uranium, into the environment, affects ecosystems and public health. These metals can be separated from aqueous solutions by various processes, where among these methods, adsorption was found to be highly efficient, with a preference that renewable and biodegradable polysaccharides be exploited as the sorbents.

The simple addition of the aqueous polysaccharide solution – of I and K from the carrageenan family, which each contain hydroxyl and ester sulfate groups, X with hydroxyl and carboxylic acid groups, and G with hydroxyl groups only – to  $\text{UO}_2^{2+}$  solutions successfully removed the  $\text{UO}_2^{2+}$ . It was found that the structures and the functional groups on the polysaccharide backbone affected the sorption efficiency, which decreased in the order of  $X > K > I/G$ . It was also found that lowering the acidity in the system decreased the sorption efficiencies with all of the tested polysaccharides due to protonation of the active sites. Furthermore, reducing the ratio between the amount of  $\text{UO}_2^{2+}$  and the amount of polysaccharide, whether by reducing the amount of  $\text{UO}_2^{2+}$  or by increasing the amount of polysaccharide, increased the sorption efficiencies with all the polysaccharides. Of all the concentrations measured, 0.03 g polysaccharide with 700 mg per L  $\text{UO}_2^{2+}$  was found to be the ratio that provided the maximum adsorption efficiency.

FTIR analysis confirmed that  $\text{UO}_2^{2+}$  was adsorbed *via* the hydroxyl groups to all of the polysaccharides, and in addition, *via* the carboxylic groups to X and *via* the sulfate ester groups to I and K. SEM-EDS analysis also verified the presence of  $\text{UO}_2^{2+}$  in the polysaccharide, and the uranium contents were in line with those of the sorption experiments. Moreover, TGA thermograms of the polysaccharides, before and after adsorption, showed that the  $\text{UO}_2^{2+}$  was adsorbed into the polysaccharide. In addition, it indicated the presence of a change in the structure of the material where the residue obtained after adsorption was larger than before the adsorption, suggesting the presence of an inorganic substance in the residue, most likely  $\text{UO}_2^{2+}$ .

Rheological measurements that were performed for the aqueous polysaccharide solution with and without  $\text{UO}_2^{2+}$  showed that the viscosity decreased sharply for all of the solutions that contained  $\text{UO}_2^{2+}$ , exhibiting Newtonian behaviour. Furthermore, the addition of  $\text{UO}_2^{2+}$  to the polysaccharides lowered both the elasticity model- $G'$  and the viscosity module- $G''$ . These findings again indicate the presence of electrostatic repulsion due to the adsorption of the  $\text{UO}_2^{2+}$  and the resultant increased distance that was obtained between the polysaccharide chains.

## Author contributions

OL-O, conceptualization, investigation, experiment design, methodology, validation, formal analysis, and writing – original draft, writing – review and editing and supervision; OP-T, conceptualization, investigation, validation, formal analysis, investigation, writing – original draft, writing – review and editing and supervision; YA, conducted the sorption



experiments; AW, conceptualization, methodology, investigation, writing – original draft, writing – review and editing, supervision, and project administration.

## Conflicts of interest

There are no conflicts to declare.

## Notes and references

- 1 A. C. Miller, *Depleted Uranium: Properties, Uses and Health Consequences*, CRC Press, Boca Raton, 1st edn, 2006, DOI: [10.1201/9781420004564](https://doi.org/10.1201/9781420004564).
- 2 M. Betti, Civil use of depleted uranium, *J. Environ. Radioact.*, 2003, **64**(2–3), 113–119.
- 3 A. Kausar and H. N. Bhatti, *J. Chem. Soc. Pak.*, 2013, **35**(3), 1041–1052.
- 4 J. Li and Y. Zhang, *Procedia Environ. Sci.*, 2012, **13**, 1609–1615.
- 5 D. Brugge and V. Buchner, *Rev. Environ. Health*, 2011, **26**(4), 231–249.
- 6 P. Kurttio, A. Harmoinen, H. Saha, L. Salonen, Z. Karpas, H. Komulainen and A. Auvinen, *Am. J. Kidney Dis.*, 2006, **47**(6), 972–982.
- 7 G. Björklund, Y. Semenova, L. Pivina, M. Dadar, M. M. Rahman, J. Aaseth and S. Chirumbolo, *Arch. Toxicol.*, 2020, **94**(5), 1551–1560.
- 8 R. Pereira, S. Barbosa and F. P. Carvalho, *Environ. Geochem. Health*, 2014, **36**(2), 285–301.
- 9 P. Henner, Bioaccumulation of Radionuclides and Induced Biological Effects in situations of chronic exposure of ecosystems a uranium case study, in *Loads and Fate of Fertilizer Derived Uranium*, ed. L. J. De Kok and E. Schnug, Backhuys Publishers Leiden, The Netherlands, 2008, pp. 23–33.
- 10 P. D. Bhalara, D. Punetha and K. Balasubramanian, *J. Environ. Chem. Eng.*, 2014, **2**(3), 1621–1634.
- 11 M. Dulama, M. Iordache and M. Deneanu, *Proceedings of NUCLEAR 2013 the 6th Annual International Conference on Sustainable Development through Nuclear Research and Education. Part 3/3*, 2013, pp. 80–86.
- 12 X. Yi, Z. Xu, Y. Liu, X. Guo, M. Ou and X. Xu, *RSC Adv.*, 2017, **7**(11), 6278–6287.
- 13 J. Bai, X. Ma, H. Yan, J. Zhu, K. Wang and J. Wang, *Microporous Mesoporous Mater.*, 2020, **306**, 110441, DOI: [10.1016/j.micromeso.2020.110441](https://doi.org/10.1016/j.micromeso.2020.110441).
- 14 L. Kong, Y. Ruan, Q. Zheng, M. Su, Z. Diao, D. Chen, L. Hou, X. Chang and K. Shih, *J. Hazard. Mater.*, 2020, **382**, 120784, DOI: [10.1016/j.jhazmat.2019.120784](https://doi.org/10.1016/j.jhazmat.2019.120784).
- 15 K. Shakir, A. F. Elkafrawy, H. F. Ghoneimy, S. G. E. Beheir and M. Refaat, *Water Res.*, 2010, **44**(5), 1449, DOI: [10.1016/j.watres.2009.10.029](https://doi.org/10.1016/j.watres.2009.10.029).
- 16 C. Aldrich and D. Feng, *Miner. Eng.*, 2010, **13**(10–11), 1129–1138.
- 17 P. Li, P. Chen, G. Wang, L. Wang, X. Wang, Y. Lia, W. Zhanga, H. Jianga and H. Chen, *Chem. Eng. J.*, 2020, **393**, 124819, DOI: [10.1016/j.cej.2020.124819](https://doi.org/10.1016/j.cej.2020.124819).
- 18 A. Mellah, S. Chegrouche and M. Barkat, *Hydrometallurgy*, 2007, **85**(2–4), 163–171.
- 19 M. Abubakar, M. N. Tamin, M. A. Saleh, M. B. Uday and N. Ahmad, *Ceram. Int.*, 2016, **42**(7), 8212–8220.
- 20 M. G. Torkabad, A. R. Keshtkar and S. J. Safdari, *Prog. Nucl. Energy*, 2017, **94**, 93–100.
- 21 A. Zaheri, A. Moheb, A. Keshtkar and A. Shirani, *J. Environ. Health Sci. Eng.*, 2010, **7**(5), 423–430.
- 22 D. Lakherwal, *International Journal of Environmental Research and Development*, 2014, **4**(1), 41–48.
- 23 B. Chen, J. Wang, L. Kong, X. Mai, N. Zheng, Q. Zhong, J. Liang and D. Chen, *Colloids Surf., A*, 2017, **520**, 612–621.
- 24 Y. Tan, L. Li, H. Zhang, D. Ding, Z. Dai, J. Xue, J. Liu, N. Hu and Y. Wang, *J. Radioanal. Nucl. Chem.*, 2018, **317**(2), 811–824.
- 25 T. S. Anirudhan and P. G. Radhakrishnan, *J. Environ. Radioact.*, 2009, **100**(3), 250–257.
- 26 M. Tsezos and B. Volesky, *Biotechnol. Bioeng.*, 1981, **23**(3), 583–604.
- 27 T. Tatarchuk, A. Shyichuk, I. Mironyuk and Mu. Naushad, *J. Mol. Liq.*, 2019, **293**, 111563, DOI: [10.1016/j.molliq.2019.111563](https://doi.org/10.1016/j.molliq.2019.111563).
- 28 F. Veglio and F. Beolchini, *Hydrometallurgy*, 1997, **44**(3), 301–316.
- 29 N. K. Gupta, A. Sengupta, A. Gupta, J. R. Sonawane and H. Sahoo, *J. Environ. Chem. Eng.*, 2018, **6**(2), 2159–2175.
- 30 M. Rinaudo, *Polym. Int.*, 2008, **57**(3), 397–430.
- 31 *Food Polysaccharides and Their Applications*, ed. A. M. Stephen, G. O. Phillips and P. A. Williams, Taylor & Francis Group, CRC Press, Boca Raton, 2nd edn, 2016.
- 32 G. Franz, *Planta Med.*, 1989, **55**(6), 493–497.
- 33 F. Freitas, V. D. Alves and M. A. Reis, *Polysaccharides*, 2015, 2017–2043.
- 34 Y. Na, J. Lee, S. H. Lee, P. Kumar, J. H. Kim and R. Patel, *Polym.-Plast. Technol. Mater.*, 2020, **59**(16), 1770–1790.
- 35 G. Crini, *Prog. Polym. Sci.*, 2005, **30**(1), 38–70.
- 36 J. Wang and C. Chen, *Biotechnol. Adv.*, 2009, **27**(2), 195–226.
- 37 A. M. Marqués, R. Bonet, M. D. Simon-Pujol, M. C. Fusté and M. F. Congregado, *Appl. Microbiol. Biotechnol.*, 1990, **34**(3), 429–431.
- 38 S. K. Kazy, P. Sar and S. F. D'Souza, *Biorem. J.*, 2008, **12**(2), 47–57.
- 39 T. Sakaguchi, A. Nakajima and T. Horikoshi, *Nippon Kagaku Kaishi*, 1979, **53**, 788–792.
- 40 C. Gok and S. Aytas, *J. Hazard. Mater.*, 2009, **168**(1), 369–375.
- 41 R. A. Muzzarelli, *Carbohydr. Polym.*, 2011, **84**(1), 54–63.
- 42 Y. Liu, Y. Liu, X. Cao, R. Hua, Y. Wang, C. Pang, M. Hua and X. Li, *J. Radioanal. Nucl. Chem.*, 2011, **290**(2), 231–239.
- 43 G. Wang, J. Liu, X. Wang, Z. Xie and N. Deng, *J. Hazard. Mater.*, 2009, **168**(2–3), 1053–1058.
- 44 L. C. B. Stopa and M. Yamaura, *Int. J. Nucl. Energy Sci. Technol.*, 2010, **5**(4), 283–289.
- 45 E. Piron and A. Domard, *Int. J. Biol. Macromol.*, 1997, **21**(4), 327–335.
- 46 E. Piron and A. Domard, *Int. J. Biol. Macromol.*, 1998, **22**(1), 33–40.
- 47 B. S. Savvin, *Talanta*, 1961, **8**, 673–685.



- 48 O. Levy-Ontman, C. Yanay, O. Paz Tal and A. Wolfson, *Mater. Today Commun.*, 2022, **32**, 104111, DOI: [10.1016/j.mtcomm.2022.104111](https://doi.org/10.1016/j.mtcomm.2022.104111).
- 49 C. M. Iain, Conformational Origins of Polysaccharides Solutions and Gel Properties, *Industrial Gums-Polysaccharides and Their Derivatives*, ed. R. L. Whistler and J. N. Bemiller, Academic Press, San Diego, 1993, pp. 21–52.
- 50 R. P. Millane, R. Chandrasekaran, S. Arnott and I. C. Dea, *Carbohydr. Res.*, 1998, **182**, 1–17.
- 51 O. Levy-Ontman, C. Yanay, O. Paz Tal and A. Wolfson, *J. Polym. Environ.*, 2023, **31**, 2321–2333.
- 52 A. Chetouani, N. Follain, S. Marais, C. Rihouey, M. Elkolli, M. Bounekhel, D. Benachour and D. LeCerf, *Int. J. Biol. Macromol.*, 2017, **97**, 348–356.
- 53 G. Sen, S. Mishra, U. Jha and S. Pal, *Int. J. Biol. Macromol.*, 2010, **47**, 164–170.
- 54 D. Mudgil, S. Barak and B. S. Khatkar, *Int. J. Biol. Macromol.*, 2012, **50**, 1035–1039.
- 55 V. Pascal, R. Besson and C. Schaffer-Lequart, *J. Agric. Food Chem.*, 2004, **52**(25), 7457–7463.
- 56 F. N. Jumaah, N. Mobarak, A. Ahmad, M. A. Ghani and M. Y. A. Rahman, *Ionics*, 2014, **21**(5), 1311–1320.
- 57 S. Karthikeyan, S. Selvasekarapandian, M. Premalatha, S. Monisha, G. Boopathi, G. Aristatil, A. Arun and S. Madeswaran, *Ionics*, 2016, **23**, 2775–2780.
- 58 V. L. Campo, D. F. Kawano, D. B. da Silva and I. Carvalho, *Carbohydr. Polym.*, 2009, **77**, 167–180.
- 59 Z. Wang, J. Wu, L. Zhu and X. Zhan, *Carbohydr. Polym.*, 2017, **157**, 521–526.
- 60 P. S. Gils, D. Ray and P. K. Sahoo, *Int. J. Biol. Macromol.*, 2009, **45**(4), 364–371.
- 61 J. Čejka, Infrared spectra and thermal analysis of the uranyl minerals, in *Uranium: Mineralogy, Geochemistry and the Environment*, ed. P. C. Burns and R. Finch, Rev. Mineral, 1999, vol. 38, pp. 521–622.
- 62 A. P. Ramos, R. R. Goncalves, O. A. Serra, M. E. D. Zaniquelli and K. Wong, *J. Lumin.*, 2007, **127**, 461–468.
- 63 L. Fuks, I. Herdzik-Koniecko, H. Polkowska-Motrenko and A. Oszczak, *Int. J. Environ. Sci. Technol.*, 2018, **15**, 2657–2668.
- 64 C. G. Mothé and M. A. Rao, *Thermochim. Acta*, 2000, **357–358**, 9–13.
- 65 D. K. Mishra, J. Tripathy and K. Behari, *Carbohydr. Polym.*, 2008, **71**, 524–534.
- 66 M. Vincekovic, A. Pustak, L. Tusek-Bozic, F. Liu, G. Ungar, M. Bujan, I. Smit and N. Filipovic-Vincekovic, *J. Colloid Interface Sci.*, 2010, **341**, 117–123.
- 67 S. Ma, L. Chen, X. Liu, D. Li, N. Ye and L. Wang, *Int. J. Green Energy*, 2012, **9**, 13–21.
- 68 W. A. K. Mahmood, M. M. R. Khan and T. C. Yee, *J. Phys. Sci.*, 2014, **25**(1), 123–138.
- 69 M. Rinaudo and M. Mils, *Biopolymers*, 1978, **17**(11), 2663–2678.
- 70 P. S. Clough, D. Dollimore and P. Grundy, *J. Inorg. Nucl. Chem.*, 1969, **31**, 361–370.
- 71 L. Abate, A. Chisari, R. Maggiore and G. Siracusa, *J. Therm. Anal.*, 1983, **27**, 139–150.

